chemosensors

MDPI

Communication

High-Performance MEMS Oxygen Sensors Based on Au/TiO_2 Films

Mingzhi Jiao [1,2,3], Xiaohu Zhao [2,3,*], Xinjian He [1], Gang Wang [2,3], Wei Zhang [4], Qian Rong [4] and DucHoa Nguyen [5]

[1] School of Safety Engineering, China University of Mining and Technology, Xuzhou 221116, China; mingzhijiao@cumt.edu.cn (M.J.)
[2] State and Local Joint Engineering Laboratory of Perception Mine, China University of Mining and Technology, Xuzhou 221116, China
[3] School of Information and Control Engineering, China University of Mining and Technology, Xuzhou 221116, China
[4] Micro and Nano Sensing Corporation, Hefei 230001, China
[5] International Training Institute of Materials Science, Hanoi University of Science and Technology, Hanoi 100000, Vietnam
* Correspondence: zhaoxiaohu@cumt.edu.cn

Abstract: High-performance microelectromechanical system (MEMS) oxygen sensors were realized by successful preparation of Au nanofilms over TiO_2 thin films through successive sputtering on commercial MEMS microhotplates. Oxygen sensing performance of 3 and 6 nm thick Au over TiO_2 thin films were compared with that of pure TiO_2 thin films. It was shown that 6 nm thick Au over TiO_2 thin films have the best sensitivity toward oxygen. The prepared TiO_2 thin films were characterized using SEM, EDS, XPS, and a gas testing instrument. The results show that Au decoration has little influence on the surface morphologies of TiO_2 thin films. However, Au decoration has a strong influence on the surface properties of the composite films. The favorable performance of 6 nm Au-doped TiO_2 thin films is attributed to factors such as catalytical performance, height of Schottky contact, and number of oxygen vacancies. This work makes contributions to low power consumption and high-performance oxygen sensors for Internet of Things applications.

Keywords: oxygen sensor; titanium dioxide; gold decoration; microhotplate; thin films

Citation: Jiao, M.; Zhao, X.; He, X.; Wang, G.; Zhang, W.; Rong, Q.; Nguyen, D. High-Performance MEMS Oxygen Sensors Based on Au/TiO_2 Films. *Chemosensors* **2023**, *11*, 476. https://doi.org/10.3390/chemosensors11090476

Academic Editor: Pi-Guey Su

Received: 12 July 2023
Revised: 13 August 2023
Accepted: 21 August 2023
Published: 28 August 2023

1. Introduction

Oxygen gas is necessary for breathing. A shortage of oxygen can cause headache or even death. Thus, monitoring of concentration of oxygen gas using gas sensors is critical to human health, especially after emergency due to fire or explosion. Metal oxide semiconductor gas sensors have been widely applied to detect relevant gases such as CH_4, H_2, CO, or O_2 considering their high sensitivity, excellent stability, and low cost [1–3]. Various oxides like ZrO_2, CeO_2, and TiO_2 have been studied for oxygen sensing [4–9]. TiO_2 is one of the most important metal oxides for oxygen sensing due to its easy availability, low cost, chemical inertness, and excellent photocatalytic properties [10]. In 2000, TiO_{2-x} films were synthesized using the sol–gel and hydrogen reduction methods [8]. However, the working temperature of the prepared TiO_{2-x} film for oxygen sensing is as high as 800 °C. High temperatures result in high power consumption and possible danger of gas combustion in settings such as coal mines with high methane content. TiO_2 thin films were synthesized using the atomic layer deposition (ALD) method and the sensor worked at temperatures below 300 °C in 2019 [11]. UV-assisted oxygen sensing of TiO_2 has recently been studied, and the working temperature can be lowered down to room temperature [12,13]. Additionally, doped TiO_2 has been further studied for oxygen sensing. For example, TiO_2 nanoparticles were added to VO_x nanoflakes using a thermal decomposition-assisted hydrothermal method. The composites show excellent temperature-independent oxygen

sensing properties, which is a result of mixed valent states in VO_x [14]. N-doped TiO_2 has much lower resistance and higher sensitivity compared to undoped TiO_2, which may come from the thermionic emission conduction mechanism or tunneling current effect under completely depleted grain conditions of TiO_2 [15].

It is worth noting that most reported TiO_2 oxygen sensors are built on Al_2O_3 substrates of relatively large size. Furthermore, Al_2O_3 substrates normally lead to high power consumption when working at temperatures higher than ambient temperature. Silicon substrate-based micro TiO_2 oxygen sensors are favored compared to Al_2O_3 substrate due to their smaller sizes, lower power consumption, and easier integration with integrated circuits. For example, a TiO_2/Pd/TiO_2 layer was manufactured on a microhotplate by combining spin coating of TiO_2 and sputtering of a Pd layer. The sensor has a working range of concentrations between 0 and 20% oxygen. However, the power consumption is estimated to be 960 mW, which is quite high [16]. TiO_2 nanorod arrays were integrated on microelectrodes on silicon through an acid vapor oxidation process on a patterned strap of Ti/Pd films. The TiO_2 nanorod arrays can respond to oxygen at room temperature, though the base resistance is larger than 10 MΩ, resulting in circuit integration difficulties [17]. Furthermore, it has been reported that Au nanoparticles can activate oxygen at the Au/TiO_2 interface due to the catalytic effect of gold nanoparticles [18,19]. Au-TiO_2 composites have been reported to be sensitive to ammonia, acetaldehyde, acetone, and formaldehyde [20–22]. Nowadays, commercial microhotplates can consume around 30 mW when working at 400 °C. If high-performance oxygen-sensitive material could be combined with microhotplates, the sensors would be very good candidates for oxygen measurement in the environment or even for Internet of Things applications. Up to now, there are no reports on the integration of Au/TiO_2 films on microhotplates for oxygen sensors. The microhotplate-based oxygen sensors may be a good solution for sensor nodes of Internet of Things applications.

Sputtering is a very efficient method for depositing metal or metal oxide thin films over substrate. It can form a dense thin film with little cracking on various substrates. Additionally, it can be carried out at low temperatures in batches [16]. In this work, Au/TiO_2 films were successfully synthesized using the sputtering method on MEMS microhotplates. The sensing performance regarding oxygen was evaluated. The sensing mechanism was also studied in detail.

2. Materials and Methods

2.1. Film Deposition and Characterization

HHC1000 MEMS microhotplates were brought from HMNST (Hefei, China). Before sputtering, bare microhotplates were bonded to a ceramic package using Au wires for conduction. The Au and TiO_2 targets were 99.99% pure and used for sputtering without further treatment. The process of sputtering is illustrated in Figure 1. TiO_2 and Au films were deposited on the microhotplates in sequence to function as oxygen-sensitive films. A radio frequency table sputtering system (Hefei Jusheng Co., Hefei, China) was employed for deposition of TiO_2 or Au film. For deposition of TiO_2 film, the flow rate of Ar was 35.4 sccm, the power of RF source was 40 W, and the temperature of the stage during deposition was 400 °C. The thickness of the film was controlled by deposition time. The deposition time of TiO_2 was 2 h and finally 300 nm of TiO_2 could be obtained. For deposition of Au film, the flow rate of Ar was 35.4 sccm, the power of RF source was 50 W, and the deposition stage was at room temperature. The deposition time of Au was 15 or 30 s in order to obtain an ultrathin non-continuous Au layer over the TiO_2 layer. The thickness of the Au films was measured at 3 or 6 nm for 15 or 30 s processing.

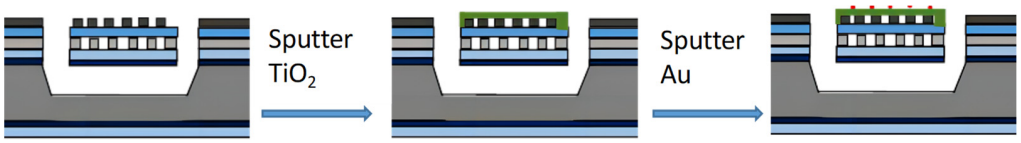

Figure 1. Fabrication process of microhotplate oxygen sensor.

The final samples obtained were named TiO_2-300 nm, TiO_2-300 nm-Au-3 nm, TiO_2-300 nm-Au-6 nm. The thickness of the thin films was measured by a Dektak XT Profilometer (Bruker, Billerica, MA, USA). The morphologies and EDS information of the films were characterized by field emission scanning electron microscopy (TESCAN MAIA3, Brno, Czech Republic). The surface chemical properties of the films were checked by an X-ray Photoelectron Spectrometer (Thermo Fisher ESCALAB 250Xi, Waltham, MA, USA).

2.2. Device Measurement

The sensing performance of the fabricated sensors was investigated in a lab-made testing system (HGS9010, designed by Hefei Micro/Nano Sensing Technology Co. Ltd., Hefei, China), which consists of a potentiometric arrangement, a testing gas chamber with a volume of 1 L, and a mixing fan. During measurement, the MEMS-based sensor was held in the gas chamber and heated using a current source (GWINSTEK, GPD-3303S, New Taipei City 236, Taiwan). The measurement was carried out in dynamic mode. The total flow rate was 500 sccm. The pure oxygen and nitrogen gas were mixed at different ratios to realize different oxygen concentrations. The resistances of the MEMS-based sensors under various temperatures and atmospheres were recorded using the testing system. To avoid the effect of the residual oxygen gas, the tests on fabricated MEMS-based sensors were conducted in the order of low to high concentrations. The sensitivity (S) of the gas sensor was calculated by $S = R_g/R_0$, where R_g is the resistance in atmosphere of mixed oxygen and nitrogen, and R_0 is the resistance in pure nitrogen, respectively. Response time and recovery time were defined according to the reported work.

3. Results

A SEM image of the whole sensor is shown in Figure 2A. The length of the square-shaped microhotplate chip is 1.0 mm. The integrated electrodes area in the middle of the square microhotplate chip is 0.1×0.1 mm^2. As seen in Figure 2B–D, there is no obvious difference in morphologies between bare TiO_2 layer and TiO_2 layers with Au decoration. This is because the thickness of the Au layer is so thin that the Au layer has little effect on the surface morphologies of TiO_2 layer.

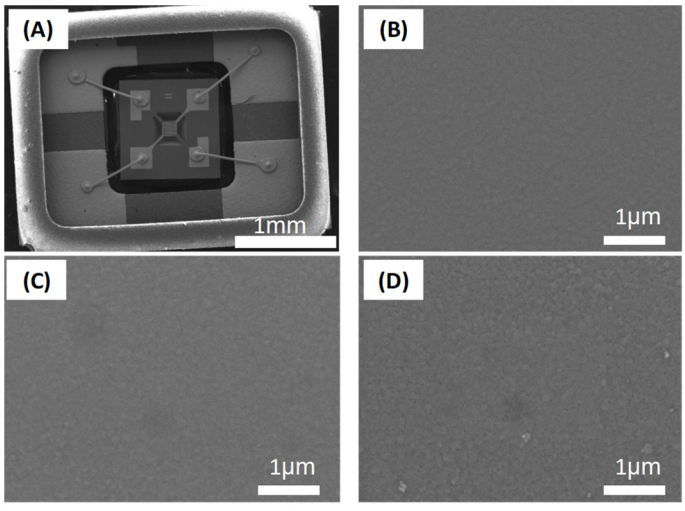

Figure 2. SEM images of oxygen sensor with TiO_2 films: (**A**) oxygen sensor chip with Au bonding wires in ceramic package, (**B**) TiO_2-300 nm, (**C**) TiO_2-300 nm-Au-3 nm, (**D**) TiO_2-300 nm-Au-6 nm.

In Figure 3A, there is no appearance of a Au element peak for pure TiO_2 thin films. The Pt peak comes from Pt electrodes underneath the TiO_2 thin films. The Au peak appears in the TiO_2-300 nm-Au-3 nm sample and contributes to 3.95% of the total weight of the sample, as shown in Figure 3B. As seen in Figure 3C, content of the Au element increases to 12.88% as the thickness of Au becomes 6 nm. The data from EDS element analysis proves that the Au element was introduced over the surface of the TiO_2 successfully.

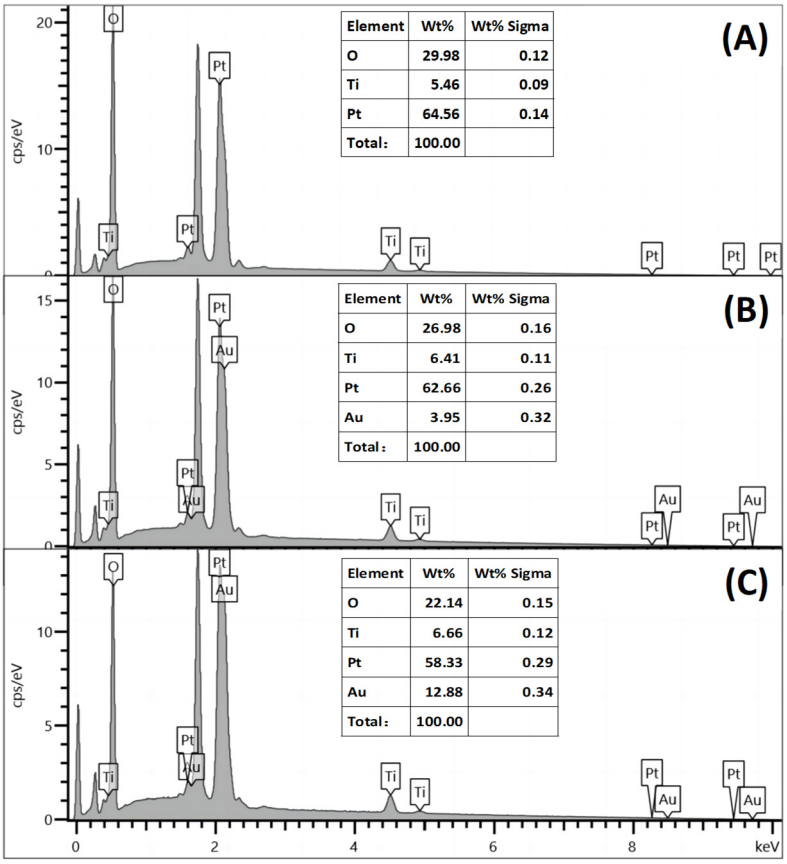

Figure 3. EDS information of three TiO_2 samples: (**A**) TiO_2-300 nm, (**B**) TiO_2-300 nm-Au-3 nm, (**C**) TiO_2-300 nm-Au-6 nm.

As seen in Figure 4A, pure TiO_2 shows a rather strong Ti element signal peak (459.34 and 464.84 eV) in the XPS diagram. Even with decoration of only a 3 nm Au layer over the TiO_2 layer, the signal of the TiO_2 element disappears considering that XPS is a surface-sensitive characterization technique. As seen in Figure 4B, no Au element signal was detected in the pure TiO_2 sample. On the contrary, the Au signal (84.15 and 87.79 eV) appears in both Au-TiO_2 samples and becomes higher for the TiO_2 composite film with the thicker Au layer. As seen in Figure 4C, the as-prepared three samples have very different signals for oxygen species. The signal at 530.54 eV belongs to lattice oxygen, while 531.69 eV belongs to vacancy oxygen and 532.34 eV belongs to OH oxygen. Pure TiO_2 thin film has two oxygen species, lattice oxygen and OH oxygen, which originate from TiO_2 and surface adsorption of water molecules in the air. TiO_2-300 nm-Au 3 nm shows no distinct lattice oxygen peak, which is the result of coverage of the surface Au layer on the surface of the TiO_2. The oxygen vacancy's peak appears for this sample while it does not appear for pure TiO_2. Since Au has a strong density of electrons, this layer can attract oxygen vacancy-positive species due to its electrostatic force. TiO_2-300 nm-Au 6 nm presents a similar peak position to TiO_2-300 nm-Au 3 nm. However, the number of oxygen vacancies becomes less for TiO_2-300 nm-Au 6 nm compared to that of TiO_2-300 nm-Au 3 nm.

As shown in Figure 5A, the 300 nm TiO_2-Au 6nm sample shows the best response to oxygen among the three samples. Compared to bare TiO_2 thin films, few nm Au decoration shows great enhancement in response to oxygen gas. The TiO_2-Au 6 nm sample has the best performance for oxygen sensing of the three samples, which is due to the influence of Schottky contact and oxygen vacancy. Figure 5B shows that the oxygen concentration and response have a linear relationship.

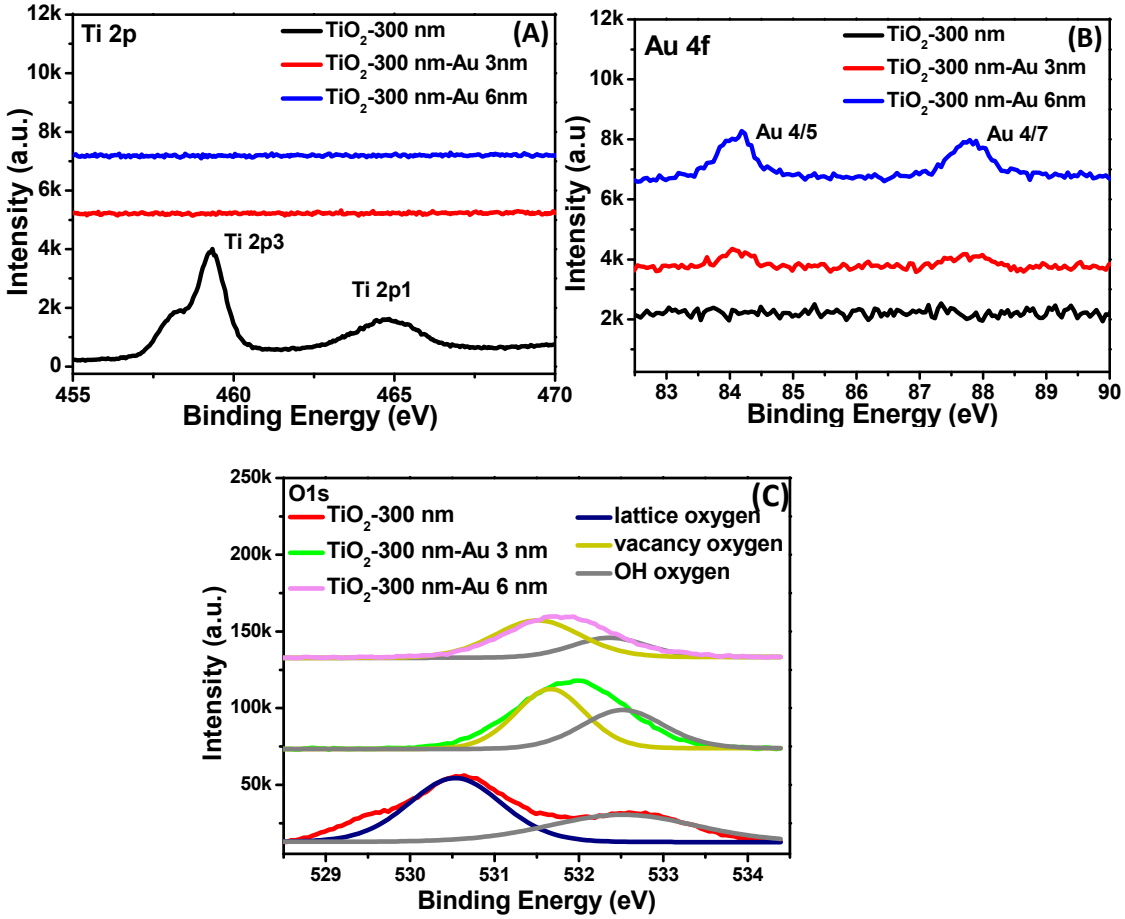

Figure 4. XPS data of three TiO_2-Au samples: (**A**) Ti 2p, (**B**) Au 4f, (**C**) O1s.

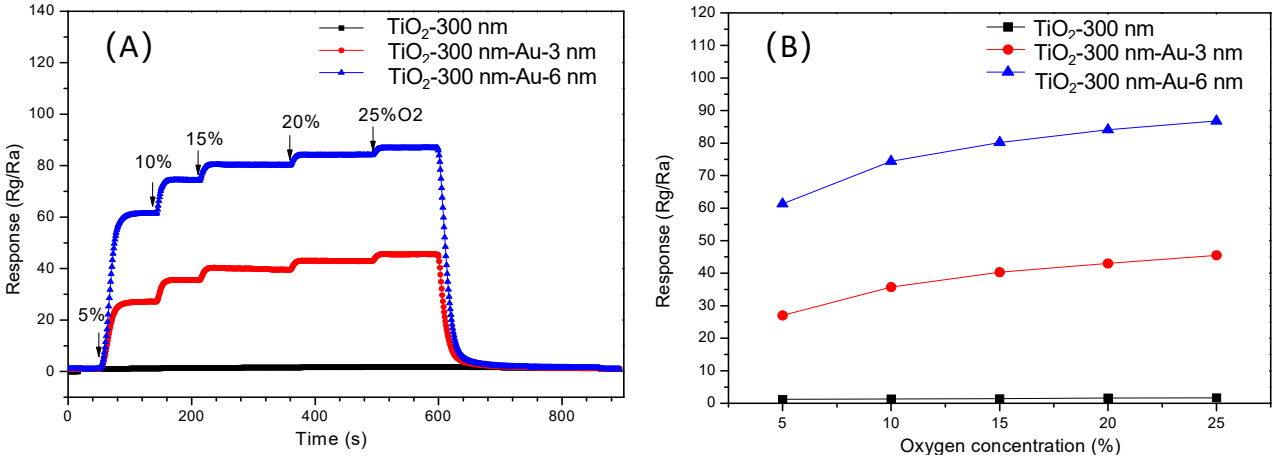

Figure 5. (**A**) Dynamic response curve toward 5–25% oxygen of different TiO_2 thin film samples; (**B**) response of different TiO_2 sample toward oxygen of various concentrations.

As shown in Table 1, our Au-TiO_2 thin films exhibit superior performance with other related works. The response time and recovery time of our samples are also shorter than those of TiO_2 nanotubes by anodic oxidation. Considering that our samples can be obtained in a facial and batch-scale way, our TiO_2 oxygen sensors are ready for commercial production with comparable performance at lower costs.

Table 1. Comparison of performance of different TiO_2 oxygen sensors.

Materials	Preparation Method	Working Temperature/°C	Oxygen Concentration (%)	Sensitivity R_g/R_0	Response Time/s	Recovery Time/s	Reference
TiO_2-VO_x	Thermal deposition and hydrothermal	500	0.01	1.32	~4	~8	[14]
TiO_2-Pt	Plasma electrolytic oxidation and sputtering	30	10	2	150	420	[23]
TiO_2-10%ZrO_2 thin film	Inkjet printing	400	5	2.2	10	28	[24]
TiO_2 nanotube	Anodic oxidation	100	4	160	500	1000	[9]
TiO_2 nanorods	Glancing angle e-beam evaporation	Room temperature under UV	0.1	74	360	-	[13]
TiO_2/Pd/TiO_2	Sol–gel and sputtering	252	4	1.16	-	-	[16]
TiO_2-300 nm-Au-6 nm	Sputtering	400	5	61.3	37	40	This work

4. Discussion

The main sensing mechanism of Au-TiO_2 nanofilms to oxygen is attributed to three parts: the catalytical effect of Au, electrical effect originating from the Schottky contact effect from Au-TiO_2, and the oxygen vacancy effect from TiO_2. The catalytical effect of Au is often referred to as the spill-over effect. Briefly speaking, Au, as a noble metal catalyst, can lower the activation energy of dissociation of oxygen molecules and facilitate the dissociation of oxygen molecules into oxygen atoms, making oxygen atom chemisorption onto the surface of TiO_2 easier. This effect increases the effective concentration of reactive oxygen species so as to enhance the sensitivity of Au/TiO_2 to oxygen gas, as seen in Figure 6A. At the same time, an increase in Au content on the surface enhances the Schottky contact effect over the surface due to the creation of more Schottky barriers, thus increasing the response, as shown in Figure 6B.

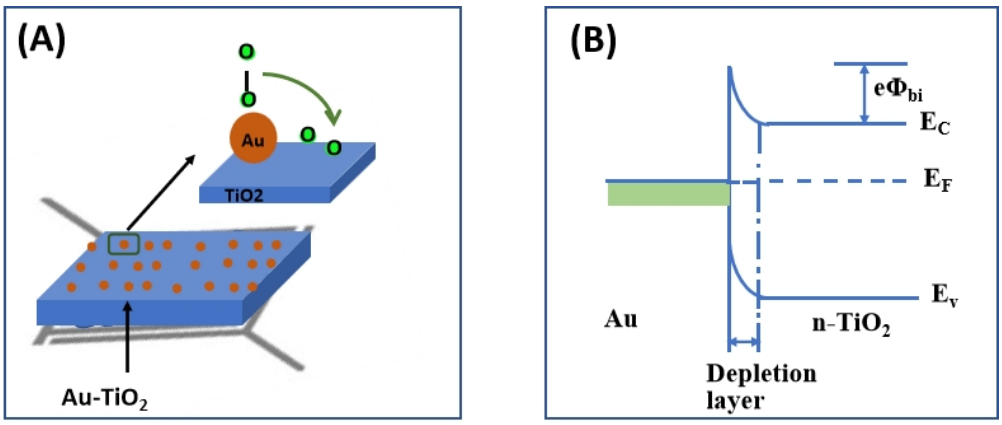

Figure 6. Diagram of sensing mechanism of the Au-TiO_2 composite films originating directly from the Au layer. (**A**) Spill-over effect of surface Au over TiO_2 layer; (**B**) Schottky contact effect between Au and TiO_2 layer.

The reaction between the O_2 and oxygen vacancies can be written as the following equation:

$$2Vo^{\cdot\cdot} + O_2 \rightarrow O_o + 4h^{\cdot} \quad (1)$$

The response of the Au-TiO_2 nanofilm oxygen sensor is influenced by the concentration of oxygen vacancies in the TiO_2 film. The Au layer on the surface generally decreases the ratio of oxygen vacancies over the whole component on the Au-TiO_2 surface, thus having a

negative effect on the response of the sample. The final response is a combination of the spill-over effect of Au, Schottky effect of Au/TiO_2, and oxygen vacancies effect of TiO_2. As shown from the results, TiO_2-300 nm-Au-6 nm has higher response to oxygen than that of TiO_2-300 nm-Au-3 nm.

5. Conclusions

It has been shown that nanometer-thick Au thin films can be added over TiO_2 thin films on microhotplate substrates to greatly promote the oxygen-sensing performance of the thin films. In our experiments, the sensing performance of 3 and 6 nm thick Au over TiO_2 thin films were compared with that of pure TiO_2 thin films. It was shown that TiO_2-300 nm-Au-6 nm has the best sensitivity toward oxygen. The best performance of TiO_2-300 nm-Au-6 nm is due to the contributions of the combination of spill-over of Au, the Schottky contact of Au-TiO_2, and the oxygen vacancy effect of TiO_2. TiO_2-300 nm-Au-3 nm has more oxygen vacancies than TiO_2-300 nm-Au-6 nm. However, TiO_2-300 nm-Au-6 nm has stronger spill-over and Schottky effects. Overall, TiO_2-300 nm-Au-6 nm has better performance than TiO_2-300 nm-Au-3 nm. Our sensor, based on TiO_2-300 nm-Au-6 nm, has a response value of 61.3 to 5% oxygen. The response time and recovery time to 5% oxygen are 37 and 40 s. The performance of our best sensor is superior to most reported TiO_2 sensors. Considering the facial and batch production nature of our methods, the oxygen sensor proposed is very promising for commercial applications.

Author Contributions: Conceptualization, M.J.; methodology, M.J., Q.R. and W.Z.; software, Q.R. and X.H.; validation, Q.R. and X.Z.; formal analysis, M.J., W.Z. and G.W; investigation, G.W.; resources, X.Z.; data curation, M.J. and X.H.; preparation, M.J. and X.H.; writing—review and editing, G.W., D.N. and X.H.; visualization, G.W. and D.N.; supervision, D.N.; project administration, D.N. and W.Z.; funding acquisition, X.Z. All authors have read and agreed to the published version of the manuscript.

Funding: This research is supported by the Fundamental Research Funds for the Central Universities (No.:2020ZDPY0223).

Institutional Review Board Statement: Not applicable.

Informed Consent Statement: Not applicable.

Data Availability Statement: Not applicable.

Acknowledgments: The Material Analysis and Test Center in China University of Mining and Technology University are thanked for the technical support.

Conflicts of Interest: The authors declare no conflict of interest.

References

1. Jiao, M.; Van Duy, N.; Chien, N.V.; Hoa, N.D.; Van Hieu, N.; Hjort, K.; Nguyen, H. On-Chip Growth of Patterned ZnO Nanorod Sensors with PdO Decoration for Enhancement of Hydrogen-Sensing Performance. *Int. J. Hydrogen Energy* **2017**, *42*, 16294–16304. [CrossRef]
2. Jiao, M.; Chen, X.Y.; Hu, K.X.; Qian, D.Y.; Zhao, X.H.; Ding, E.J. Recent Developments of Nanomaterials-Based Conductive Type Methane Sensors. *Rare Met.* **2021**, *40*, 1515–1527. [CrossRef]
3. Ramamoorthy, R.; Dutta, P.K.; Akbar, S.A. Oxygen Sensors: Materials, Methods, Designs and Applications. *J. Mater. Sci.* **2003**, *38*, 4271–4282. [CrossRef]
4. Phan, T.T.; Tosa, T.; Majima, Y. 20-nm-Nanogap Oxygen Gas Sensor with Solution-Processed Cerium Oxide. *Sens. Actuators B Chem.* **2021**, *343*, 130098. [CrossRef]
5. Ramshanker, N.; Ganapathi, K.L.; Bhat, M.S.; Mohan, S. RF Sputtered CeO_2 Thin Films-Based Oxygen Sensors. *IEEE Sens. J.* **2019**, *19*, 10821–10828. [CrossRef]
6. Mokrushin, A.S.; Simonenko, E.P.; Simonenko, N.P.; Bukunov, K.A.; Sevastyanov, V.G.; Kuznetsov, N.T. Gas-Sensing Properties of Nanostructured CeO_2-$XZrO_2$ Thin Films Obtained by the Sol-Gel Method. *J. Alloys Compd.* **2019**, *773*, 1023–1032. [CrossRef]
7. Yamada, T.; Kubota, Y.; Makinose, Y.; Suzuki, N.; Nakata, K.; Terashima, C.; Matsushita, N.; Okada, K.; Fujishima, A.; Katsumata, K.I. Single Crystal ZrO_2 Nanosheets Formed by Thermal Transformation for Solid Oxide Fuel Cells and Oxygen Sensors. *ACS Appl. Nano Mater.* **2019**, *2*, 6866–6873. [CrossRef]
8. Zheng, L.; Xu, M.; Xu, T. TiO_{2-x} Thin Films as Oxygen Sensor. *Sens. Actuators B Chem.* **2020**, *66*, 28–30. [CrossRef]

9. Lu, H.F.; Li, F.; Liu, G.; Chen, Z.G.; Wang, D.W.; Fang, H.T.; Lu, G.Q.; Jiang, Z.H.; Cheng, H.M. Amorphous TiO_2 Nanotube Arrays for Low-Temperature Oxygen Sensors. *Nanotechnology* **2008**, *19*, 405504. [CrossRef]
10. Sharma, R.K.; Bhatnagar, M.C.; Sharma, G.L. Influence of Doping on Sensitivity and Response Time of TiO_2 Oxygen Gas Sensor. *Rev. Sci. Instrum.* **2000**, *71*, 1500–1504. [CrossRef]
11. Mokrushin, A.S.; Simonenko, E.P.; Simonenko, N.P.; Akkuleva, K.T.; Antipov, V.V.; Zaharova, N.V.; Malygin, A.A.; Bukunov, K.A.; Sevastyanov, V.G.; Kuznetsov, N.T. Oxygen Detection Using Nanostructured TiO_2 Thin Films Obtained by the Molecular Layering Method. *Appl. Surf. Sci.* **2019**, *463*, 197–202. [CrossRef]
12. Jyothilal, H.; Shukla, G.; Walia, S.; Bharath, S.P.; Angappane, S. UV Assisted Room Temperature Oxygen Sensors Using Titanium Dioxide Nanostructures. *Mater. Res. Bull.* **2021**, *140*, 111324. [CrossRef]
13. Wang, Y.; Lai, X.; Liu, B.; Chen, Y.; Lu, Y.; Wang, F.; Zhang, L. UV-Induced Desorption of Oxygen at the TiO_2 Surface for Highly Sensitive Room Temperature O_2 Sensing. *J. Alloys Compd.* **2019**, *793*, 583–589. [CrossRef]
14. Raghu, A.V.; Karuppanan, K.K.; Pullithadathil, B. Highly Sensitive, Temperature-Independent Oxygen Gas Sensor Based on Anatase TiO_2 Nanoparticle Grafted, 2D Mixed Valent VO_x Nanoflakelets. *ACS Sens.* **2018**, *3*, 1811–1821. [CrossRef] [PubMed]
15. Buono, C.; Desimone, M.; Schipani, F.; Aldao, C.M.; Vignatti, C.I.; Morgade, C.I.N.; Cabeza, G.F.; Garetto, T.F. N-Doping Effects on the Oxygen Sensing of TiO_2 Films. *J. Electroceramics* **2018**, *40*, 72–77. [CrossRef]
16. Wang, H.; Wang, J.; Chen, L.; Yao, Y.; Sun, Q.; Qunming, Z. Integrated Microoxygen Sensor Based on Nanostructured TiO_2 Thin Films. *Micro Nano Lett.* **2015**, *10*, 597–602. [CrossRef]
17. Wang, H.; Sun, Q.; Yao, Y.; Li, Y.; Wang, J.; Chen, L. A Micro Sensor Based on TiO_2 Nanorod Arrays for the Detection of Oxygen at Room Temperature. *Ceram. Int.* **2016**, *42*, 8565–8571. [CrossRef]
18. Liang, L.; Yin, J.; Bao, J.; Cong, L.; Huang, W.; Lin, H.; Shi, Z. Preparation of Au Nanoparticles Modified TiO_2 Nanotube Array Sensor and Its Application as Chemical Oxygen Demand Sensor. *Chin. Chem. Lett.* **2019**, *30*, 167–170. [CrossRef]
19. Siemer, N.; Lüken, A.; Zalibera, M.; Frenzel, J.; Muñoz-Santiburcio, D.; Savitsky, A.; Lubitz, W.; Muhler, M.; Marx, D.; Strunk, J. Atomic-Scale Explanation of O_2 Activation at the Au-TiO_2 Interface. *J. Am. Chem. Soc.* **2018**, *140*, 18082–18092. [CrossRef]
20. Ren, H.; Weng, H.; Huang, J.; Lu, X.; Joo, S.W. Synthesis of Au Nanoparticle-Modified Porous TiO_2 Nano-spheres for Detection of Toxic Volatile Organic Vapors. *J. Alloys Compd.* **2022**, *919*, 165843. [CrossRef]
21. Zhang, S.; Zhao, L.; Huang, B.; Li, X. Enhanced Sensing Performance of Au-Decorated TiO_2 Nanospheres with Hollow Structure for Formaldehyde Detection at Room Temperature. *Sens. Actuators B Chem.* **2022**, *358*, 131465. [CrossRef]
22. Mintcheva, N.; Srinivasan, P.; Rayappan, J.B.B.; Kuchmizhak, A.A.; Gurbatov, S.; Kulinich, S.A. Room-Temperature Gas Sensing of Laser-Modified Anatase TiO_2 Decorated with Au Nanoparticles. *Appl. Surf. Sci.* **2020**, *507*, 145169. [CrossRef]
23. Engelkamp, B.; Schierbaum, K. Oxygen Sensing of Pt/Peo-TiO_2 in Humid Atmospheres at Moderate Temperatures. *Sensors* **2021**, *21*, 2558. [CrossRef]
24. Simonenko, E.P.; Mokrushin, A.S.; Simonenko, N.P.; Voronov, V.A.; Kim, V.P.; Tkachev, S.V.; Gubin, S.P.; Sevastyanov, V.G.; Kuznetsov, N.T. Ink-Jet Printing of a TiO_2–10%ZrO_2 Thin Film for Oxygen Detection Using a Solution of Metal Alkoxoacetylacetonates. *Thin Solid Films* **2019**, *670*, 46–53. [CrossRef]